Highly compact vector bending sensor with microfiber-assisted Mach-Zehnder interferometer

Ting Liu, Hao Zhang, Bo Liu, Xu Zhang, Haifeng Liu, Chao Wang

***Abstract*—A low-cost and highly compact fiber-optic component is proposed and experimentally demonstrated for vector bending sensing. A segment of microfiber tapered from standard single-mode fibers (SMFs) is spliced between two SMFs with pre-designed lateral offset to construct a sandwich type Mach-Zehnder interferometer of 243.32 μm in length. Sensing performances of the proposed vector bending sensor is theoretically analyzed in detail. As the applied curvature increases from 0.3873 m^{-1} to 3.0 m^{-1}, the transmission spectra of the proposed sensor show distinct linear wavelength shift sensitivities for different directions, the maximum of which is up to 3.419 nm/m^{-1}. Besides, temperature test indicates that the proposed sensor possesses a low temperature cross sensitivity of 33.71 pm/°C, which ensures its applicability for practical uses in temperature-fluctuated environment. Hence, our proposed vector bending sensor possesses such desirable merits as high sensitivity, compact size, low thermal crosstalk, low cost and orientation-dependent spectral response.**

***Index Terms*—Curvature measurement; Mach-Zehnder interferometer; Vector bending sensor ; Lateral core-offset**

I. Introduction

In recent decades, the demand for high precision curvature measurement has been consistently growing in the fields of mechanical engineering, crack monitoring, and aerospace detection, etc. Due to their distinguished advantages such as high sensitivity, fast response, structure flexibility, and immunity to electromagnetic interference, and thanks to the revolutionized development of optical fiber technology, a good variety of fiber-optic devices, such as fiber gratings [1-3], Fabry-Pérot cavity [4], and Mach-Zehnder interferometers (MZIs) [5-7], have been proposed for bending sensing applications in the past decades.

Nevertheless, the most commonly employed fiber grating sensors are normally susceptible to environmental thermal state, which severely degrades the sensor performances in terms of measurement reliability and accuracy [8]. And moreover, device size is another issue that limits the deployment of grating sensors on the occasions where only miniaturized devices are applicable for practical use. Fabry-Pérot fiber sensors [9, 10] have also been intensively investigated for their simple structure and ease of fabrication; however, their bending sensitivities are relatively lower compared with fiber grating sensors. As a promising candidate to further improve the performances of bending sensors, MZI-based fiber-optic sensors have attracted considerable research interests in recent years. In MZI-based sensing schemes, two mode-coupling fiber joints are normally employed to separate the input light and then re-combine the light at the output port, respectively. Typical methods to fabricate the mode coupling joint includes abrupt taper [11-13], core mismatching [14], and offset splicing [15], making their transmission spectral property more sensitive to the structural bending. However, due to their geometric symmetry with respect to the fiber axis, the above mentioned abrupt taper-based fiber sensors are unable to distinguish the orientation of bending. In addition, employment of special fibers would inevitably increase sensor cost and fabrication difficulty.

To eliminate the above defects, a microfiber-assisted MZI (MAMZI) sensor is proposed in this paper for highly sensitive and cost-effective vector bending measurement with good dynamic curvature range and ease of fabrication.

II. Fabrication procedure of the MAMZI and theoretical analysis

With the assistance of flame scanning technique to fabricate a tapered microfiber as well as modified charging parameters to achieve splicing between the microfiber and standard single-mode fibers (SMFs), the proposed MAMZI is fabricated according to the following procedure. Firstly, one segment of SMF is tapered to produce a thinned fiber with smooth waist transition region by employing flame scanning technique. The microfiber is cut at its waist region with a diameter of about 40 μm to 60 μm. The cleaved fiber is then spliced with the lead-in

This work was jointly supported by the National Natural Science Foundation of China under Grant Nos. 11774181, 61875091, 61727815, 11274182, and 11004110, Science & Technology Support Project of Tianjin under Grant No. 16YFZCSF00400, and the 863 National High Technology Program of China under Grant No. 2013AA014201. (Corresponding author: Hao Zhang)

T. Liu, H. Zhang, B. Liu, X. Zhang, and H. Liu are with Tianjin Key Laboratory of Optoelectronic Sensor and Sensing Network Technology, Institute of Modern Optics, Nankai University, Tianjin 300350, China. (e-mail: 1349224572@qq.com; haozhang@nankai.edu.cn; liubo@nankai.edu.cn; zhang_xu0315@sina.com; hfliu@mail.nankai.edu.cn)

C. Wang is with School of Engineering and Digital Arts, University of Kent, Canterbury CT2 7NT, United Kingdom. (e-mail: c.wang@kent.ac.uk)

SMF with pre-designed lateral offset by using a commercial fiber splicer (Fujikura FSM-60 s, Japan), and the other end of the fabricated microfiber is precisely cleaved to form a ~200-μm-long microfiber (MF), which is ultimately spliced with the lead-out SMF with the same amount of lateral offset. The detailed fabrication procedure of the MAMZI could be found in our previous study [16]. Schematic diagram of the proposed MAMZI sensor is shown in Fig. 1, where L_{MF} and D_{MF} refer to the length and diameter of the MF, respectively, and D_{off} represents lateral offset between the MF and the core regions of the lead-in and lead-out SMFs.

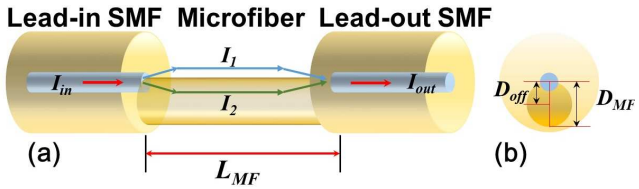

Fig 1. Schematic diagram of the proposed MAMZI-based sensor. (a) Three-dimensional diagram, (b) cross-sectional perspective.

Due to the mode mismatch between the lead-in SMF and the MF, the incident light will separate into two beams that respectively propagate through the air cavity and the MF. These two beams will re-combine at the second fiber splicing joint between the MF and the lead-out SMF for similar reason. Here, the light intensity of the incident light and the two beam branches are specified by I_{in}, I_1, and I_2, respectively. When the two beams re-combine at the second fiber splicing joint, optical interference occurs due to the optical path difference (OPD) between them. The transmission light intensity I_{out} could be described as [5-7]

$$I_{out} = I_1 + I_2 + 2\sqrt{I_1 I_2}\cos(\Delta\varphi), \tag{1}$$

where $\Delta\varphi = \frac{2\pi(n_{MF}-n_{air})L_{MF}}{\lambda} = \frac{2\pi\Delta n_{eff}L_{MF}}{\lambda}$ refers to OPD between the two branches of light, n_{MF} and n_{air} represent effective refractive indexes of the optical modes respectively propagating through the MF and air cavity, Δn_{eff} denotes the difference between them, and λ is wavelength of the light in vacuum. According to (1), resonance dips would appear when $\Delta\varphi = (2m+1)\pi$, where m is an integer. The mth order dip λ_m could be calculated by

$$\lambda_m = 2\Delta n_{eff} L_{MF} / (2m+1). \tag{2}$$

Free spectral range (FSR) Δλ of the proposed MAMZI could be expressed as

$$\Delta\lambda = \lambda_m \lambda_{m-1} / \Delta n_{eff} L_{MF}. \tag{3}$$

Fig. 1(b) shows the cross sectional geometry of the proposed MAMZI, where the light orange and blue areas represent the SMF area and the dark yellow region corresponds to the MF region. It could be seen that the introduction of the MF with pre-designed lateral offset from the lead-in and lead-out SMFs breaks up the fiber circular symmetry. This will lead to direction-dependent bending responses contingent on the fiber cross sectional symmetry.

The vector bending sensing system is schematically illustrated in Fig. 2(a), which consists of a broadband source (BBS) that provides a broadband light output from 1250 nm to 1640 nm, an optical spectrum analyzer (OSA: Yokogawa AQ6370C) with a spectral resolution of 0.1 nm, and two settings of 360 ° rotators mounted on micro-displacement stages (MSs) with a displacement resolution of 10 μm. The lead-in and lead-out SMFs of the proposed MAMZI are straightly clamped by two copper pillars of the rotators. Fig. 2(b) gives the sketch for curvature calculation. It could be seen that the curvature of the proposed interferometric sensor could be tuned by changing the distance of two MSs.

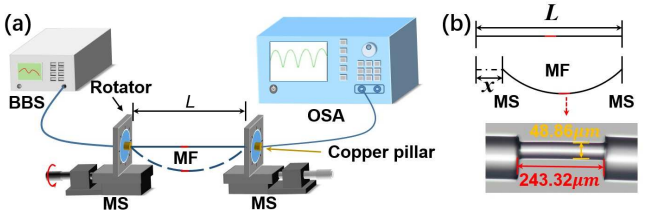

Fig. 2. (a) Experimental setup of the MAMZI-based vector bending sensing system. (b) Sketch for curvature calculation.

Curvature (C) of the proposed MAMZI sensor could be approximately evaluated by [17]

$$C = \frac{1}{R} \cong \sqrt{\frac{24x}{L^3}}, \tag{4}$$

where R represents bending radius of the MF, L is initial distance between the two MSs, and x refers to the displacement of one end with respect to its original position. In our experiment, L is 20 cm and x changes from 50 μm to 3000 μm. According to (4), the applied curvature varies from 0.3873 m^{-1} to 3.0 m^{-1}.

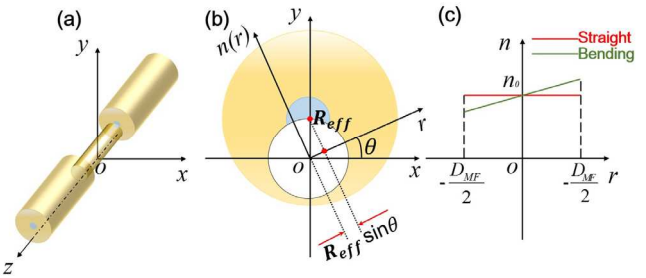

Fig. 3. (a) Unbent sensor in Cartesian coordinate system. (b) Fiber cross sectional geometry of the sensor bent in r axis. (c) Fiber cross sectional RI distribution in r axis.

As shown in Fig. 3, the bending direction is characterized by θ which is defined as the angle of the r vector with respect to $+x$ axis. When the MF is bent in r axis, the deformation-induced internal stress will cause refractive index (RI) change in the MF region through elasto-optical effect, and hence the resonance dips will shift accordingly. The cross-sectional RI distribution could be described in terms of applied curvature by the following equation [18, 19]

$$n(r) = n_0\left(1+\frac{C}{\rho}r\right), \tag{5}$$

where n_0 is the RI of the straight MF, r is the distance between the MF core center and the point under investigation, ρ is the modified elasto-optic coefficient, and $n(r)$ describes the RI

distribution in the bending direction axis. Fig. 3(c) gives the fiber cross sectional RI distribution in r axis based on (5). We concentrate on the RI variation of the effective region that supports light transmission in the MF. Since the fiber core regions of the lead-in and lead-out SMFs are very close to the MF cladding, the spectral interference dominantly results from the light beams respectively propagating through the air cavity and the cladding area of the MF. For simplicity, the displacement of this small region from the MF core center (namely the origin in Fig. 3(b)) could be regarded as R_{eff}, which is slightly smaller than $D_{MF}/2$. This implies that it is reasonable to study the RI change at the equivalent point (0, R_{eff}) in the two-dimensional Cartesian coordinate system.

As a result, n_0 equals the silica-based cladding RI of 1.444. Unlike the RI distribution in the bending direction (i.e., the r axis), the RI at point (0, R_{eff}) is no longer dependent on the distance between the origin and the point (0, R_{eff}) but on the projection of $\overrightarrow{OR_{eff}}$ in r axis. Therefore, the RI at point (0, R_{eff}) could be modified as

$$n = n_0\left(1+\frac{C}{\rho}\overrightarrow{OR_{eff}}\cdot\hat{r}\right)=n_0\left(1+\frac{C}{\rho}R_{eff}\sin\theta\right), \quad (6)$$

where n is the equivalent approximation of n_{MF}, $\hat{r}$ represents the unit vector in r axis. By substituting (6) into (2) the following expression could be acquired

$$\lambda_m(\mathrm{C}) = \frac{2\times\left[n_0\left(1+\frac{C}{\rho}R_{eff}\sin\theta\right)-n_{air}\right]\times L_{MF}}{2m+1}. \quad (7)$$

The theoretical vector bending sensitivity S in terms of the resonance dip wavelength shift in response to curvature variation could be described as:

$$S = \frac{d\lambda_m}{dC} = \frac{2n_0R_{eff}L_{MF}}{(2m+1)\rho}\sin\theta. \quad (8)$$

The above equation indicates that S should be proportional to $\sin\theta$, and this conclusion could be verified by our successive experimental results.

III. Experimental Results and Discussion

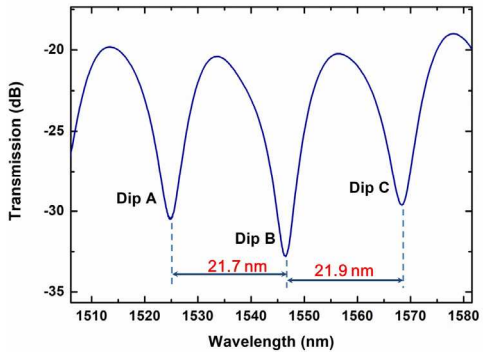

Fig. 4. Experimentally acquired transmission spectrum for FSR evaluation.

From the microscopic inset of Fig. 2(b), it could be seen that length L_{MF} and diameter D_{MF} are 243.32 μm and 48.86 μm, respectively. When the MF is initially straight, no RI variation is introduced, and according to (6) n_{MF} equals 1.444. The spectral responses around 1550 nm is investigated in our experiment. As shown in Fig. 4, dips A, B, C are selected to evaluate FSR of our proposed sensor, and the experimental results turn out to be 21.7 and 21.9 nm, which are in good accordance with the theoretical value of 22.2 nm calculated by using (3).

We have also experimentally investigated the direction-dependent bending response of the proposed MAMZI sensor, as shown in Fig. 5. Fig. 5(a) to (d) shows different spectral evolutions of dip B as the applied curvature increases from 0.3873 m^{-1} to 3.0 m^{-1} for the 0 °, 90 °, 180 ° and 270 ° directions, respectively, where the arrows point to the curvature increment directions.

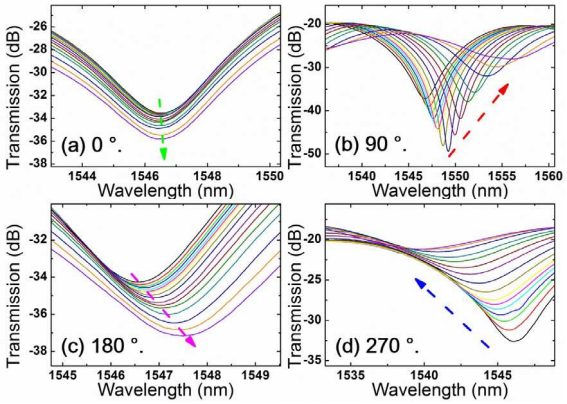

Fig. 5. Spectral evolution of dip B for different bending directions. (a) 0 °. (b)90 °. (c) 180 °. (d) 270 °

By changing the bending directions from 0 ° to 330 ° with a step of 30 °, the vector bending spectral responses have been experimentally studied, as shown in Fig. 6. Linear fit of experimental data indicates that the spectral responses are highly correlated with applied bending direction, and the maximum sensitivity reaches 3.419 nm/m^{-1} for the rotational angle of 90 °.

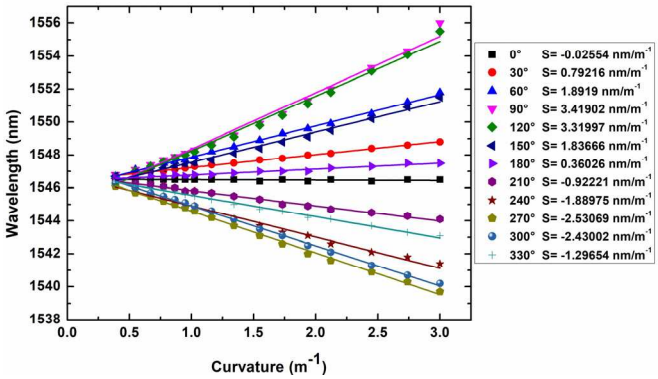

Fig. 6. Resonance dip wavelength as functions of applied curvature for different bending directions.

Fig. 7 gives bending sensitivity as a function of rotational angle. From this figure, it is apparent that there is sinusoidal relationship between these two parameters and the coefficient of determination is 0.973. This is in good agreement with our

theoretical prediction based on (8). It should be noted that, different from (8), an initial phase of 13.504 ° is present in the sinusoidally fit expression of the experimental data. This could be attributed to the fact that it is rather difficult to assure the initial rotational angle is precisely 0 ° in our experiment. Besides, there is a constant deviation of 0.24553 could also be found in the nonlinear fit result. This is because rather than maintaining a constant value, L_{MF} slightly changes during the bending process.

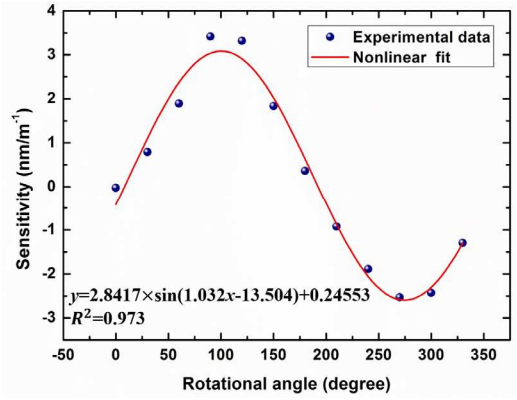

Fig. 7. Bending sensitivity as a function of rotational angle.

As an important factor that should be considered in practical applications, the temperature response of the MAMZI sensor has also been experimentally investigated within a temperature range of 25.7 to 99.9 °C, as shown in Fig. 8. It could be seen that the resonance dips show some redshift as environmental temperature increases. Linear fit indicates that the thermal sensitivity is 33.71 pm/°C, which means that the temperature cross sensitivity could be actually neglected.

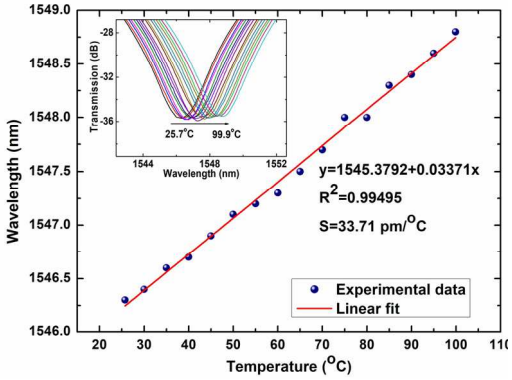

Fig. 8. Wavelength shift against temperature.

TABLE I
COMPARISON OF SENSING FEATURES BETWEEN OUR WORK AND OTHER REPORTED BENDING SENSORS

Ref.	Cur. Sens. (nm/m^{-1})	Direction	Testing range(m^{-1})	Size (mm)
[1]	0.05947	Sensitive	1.6-7.69	Not given
[3]	-0.0374	Sensitive	-20-20	Not given
[10]	0.06852	Insensitive	35-45	1.14
[14]	-2.42	Insensitive	0-1.739	41.5
Our work	3.419	Sensitive	0.3873-3	0.243

Tab. 1 gives a comparison of sensor performances of our proposed MAMZI with other related reports. It could be seen that the MAMZI sensor has an ultra-compact size with a high bending sensitivity as well as direction-dependent property.

The proposed fiber-optic vector bending sensor is endurable within a curvature measurement range up to 3.0 m^{-1}, which would be particularly suitable for micro-bending measurement occasions.

IV. CONCLUSIONS

In summary, a highly sensitive and ultra-compact vector bending sensor has been proposed and experimentally demonstrated. The introduction of MF with pre-designed lateral offset forms a MZI with an asymmetric fiber structure, leading to direction-dependent spectral responses. The resonance dip wavelength linearly shift as applied curvature increases from 0.3873 to 3.0 m^{-1}. The bending sensitivities vary from -2.530 to 3.419 nm/m^{-1} for different bending directions and there exists a sinusoidal relationship between bending sensitivity and rotational angle, which is in good agreement with our theoretical analysis. Moreover, experimental results indicate that our proposed sensor possesses a low temperature sensitivity of 33.71 pm/°C. The MAMZI-based vector bending sensor has such desirable merits as ultra-compactness, low cost, and low thermal crosstalk, making it a promising candidate for in-situ vector bending sensing applications.

REFERENCES

[1] M. Hou, K. Yang, J. He, X. Xu, S. Ju, K. Guo, and Y. Wang, "Two-dimensional vector bending sensor based on seven-core fiber Bragg gratings," *Opt. Express,* vol. 26, no. 18, pp. 23770-23781, Sep. 2018.

[2] G. M. H. Flockhart, W. N. MacPherson, J. S. Barton, J. D. C. Jones, L. Zhang, and I. Bennion, "Two-axis bend measurement with Bragg gratings in multicore optical fiber," *Opt. Lett.,* vol. 28, no. 6, pp. 387-389, Mar. 2003.

[3] K. Yang, J. He, C. Liao, Y. Wang, S. Liu, K. Guo, J. Zhou, Z. Li, Z. Tan, and Y. Wang, "Femtosecond Laser Inscription of Fiber Bragg Grating in Twin-Core Few-Mode Fiber for Directional Bend Sensing," *J. Lightwave Technol.,* vol. 35, no. 21, pp. 4670-4676, Nov. 2017.

[4] J. Kong, A. Zhou, and L. Yuan, "Temperature insensitive one-dimensional bending vector sensor based on eccentric-core fiber and air cavity Fabry-Perot interferometer," *J. Opt.,* vol. 19, no. 4, Apr. 2017.

[5] Y. Tian, Q. Chai, T. Tan, B. X. Mu, Q. Liu, Y. L. Liu, J. Ren, J. Z. Zhang, K. Oh, E. Lewis, J. Yang, Z. H. Liu, W. P. Zhang, and L. B. Yuan, "Directional Bending Sensor Based on a Dual Side-Hole Fiber Mach-Zehnder Interferometer," *IEEE Photonic Technol. Lett.,* vol. 30, no. 4, pp. 375-378, Feb. 2018.

[6] L. Zhang, W. Zhang, L. Chen, T. Yan, L. Wang, B. Wang, and Q. Zhou, "A Fiber Bending Vector Sensor Based on M-Z Interferometer Exploiting Two Hump-Shaped Tapers," *IEEE Photonic Technol. Lett.,* vol. 27, no. 11, pp. 1240-1243, Jun. 2015.

[7] S. Zhang, W. Zhang, S. Gao, P. Geng, and X. Xue, "Fiber-optic bending vector sensor based on Mach -Zehnder interferometer exploiting lateral-offset and up-taper," *Opt. Lett.,* vol. 37, no. 21, pp. 4480-4482, Nov. 2012.

[8] M. N. Ng, and K. S. Chiang, "Thermal effects on the transmission spectra of long-period fiber gratings," *Opt. Commun.,* vol. 208, no. 4-6, pp. 321-327, Jul. 2002.

[9] X. Xu, J. He, M. Hou, S. Liu, Z. Bai, Y. Wang, C. Liao, Z. Ouyan, and Y. Wang, "A Miniature Fiber Collimator for Highly Sensitive

Bend Measurements," *J. Lightwave Technol.,* vol. 36, no. 14, pp. 2827-2833, Jul. 2018.
[10] C. S. Monteiro, M. S. Ferreira, S. O. Silva, J. Kobelke, K. Schuster, J. Bierlich, and O. Frazao, "Fiber Fabry-Perot Interferometer for Curvature Sensing," *Photonic Sens.,* vol. 6, no. 4, pp. 339-344, Dec. 2016.
[11] Y. Zhao, M.-q. Chen, F. Xia, L. Cai, and X.-G. Li, "Small Curvature Sensor Based on Butterfly-Shaped Mach-Zehnder Interferometer," *IEEE Trans. on Electron Devices,* vol. 64, no. 11, pp. 4644-4649, Nov. 2017.
[12] Q. Meng, X. Dong, Z. Chen, K. Ni, and IEEE, *Simultaneous measurement of curvature and temperature based on two waist-enlarged fiber tapers and a fiber Bragg grating*, 2012.
[13] L. Niu, C.-L. Zhao, H. Gong, Y. Li, and S. Jin, "Curvature sensor based on two cascading abrupt-tapers modal interferometer in single mode fiber," *Opt. Commun.,* vol. 333, pp. 11-15, Dec. 2014.
[14] K. Tian, Y. Xin, W. Yang, T. Geng, J. Ren, Y.-X. Fan, G. Farrell, E. Lewis, and P. Wang, "A Curvature Sensor Based on Twisted Single-Mode-Multimode-Single-Mode Hybrid Optical Fiber Structure," *J. Lightwave Technol.,* vol. 35, no. 9, pp. 1725-1731, May. 2017.
[15] L. Mao, P. Lu, Z. Lao, D. Liu, and J. Zhang, "Highly sensitive curvature sensor based on single-mode fiber using core-offset splicing," *Opt. Laser Technol.,* vol. 57, pp. 39-43, Apr. 2014.
[16] B. Song, H. Zhang, B. Liu, W. Lin, and J. Wu, "Label-free in-situ real-time DNA hybridization kinetics detection employing microfiber-assisted Mach-Zehnder interferometer," *Biosens. Bioelectron.,* vol. 81, pp. 151-158, Jul. 2016.
[17] C. Zhang, J. Zhao, C. Miao, Z. Shen, H. Li, and M. Zhang, "High-sensitivity all single-mode fiber curvature sensor based on bulge-taper structures modal interferometer," *Opt. Commun.,* vol. 336, pp. 197-201, Feb. 2015.
[18] J. Sun, Y. Qi, Z. Kang, L. Ma, and S. Jian, "A Modified Bend-Resistant Multitrench Fiber With Two Gaps," *J. Lightwave Technol.,* vol. 33, no. 23, pp. 4908-4914, Dec. 2015.
[19] S. Ma, T. Ning, S. Lu, J. Zheng, J. Li, and L. Pei, "Bending-Resistant Design of a Large Mode Area Segmented Cladding Fiber With Resonant Ring," *J. Lightwave Technol.,* vol. 36, no. 14, pp. 2844-2849, Jul. 2018.

Ting Liu received the Bachelor's degree in optoelectric information science and engineering from Wuhan Institute of Technology, China, in 2017. She is currently a Master degree candidate in optical engineering at Institute of Modern Optics, Nankai University. Her research interests are mainly focused on fiber-optic sensing technology.

Hao Zhang received the Ph.D. degree in optics from Nankai University, China, in 2005. He is currently a professor at Institute of Modern Optics, Nankai University. His research interests include micro/nanostructured fiber devices, novel fiber sensors, and fiber lasers.

Bo Liu received the Ph.D. degree in optics from Nankai University, China, in 2004. He is currently a professor at Institute of Modern Optics, Nankai University. His research interests include fiber sensors, fiber-grating-based photonic devices, and interrogation systems.

Xu Zhang received the Bachelor's degree from Dalian University of technology, Liaoning, China, in 2016. She is currently a Master degree candidate in optical engineering at the Institute of Modern Optics, Nankai University. Her research interests are mainly focused on fiber-optic interferometers for biosensing.

Haifeng Liu received the Ph.D. degree in Optics from Nankai University, China, in 2016. He is currently an engineer at Institute of Modern Optics, Nankai University. His research interests include novel fiber-optic devices based on functional materials and their applications.

Chao Wang received the Ph. D. degree in Electrical and Computer Engineering from University of Ottawa, Canada, in 2011. He is currently a Senior Lecturer in the School of Engineering and Digital Arts, University of Kent, UK. His research interests lie in inter-disciplinary areas that study the interaction between Photonics and other traditional or state-of-the-art technologies in different fields, such as microwave photonics, optical communications, and biophotonics for widespread industrial, communications, biomedical and defense applications.